AIAA JOURNAL
Vol. 34, No. 6, June 1996

High-Enthalpy, Hypersonic Compression Corner Flow

S. G. Mallinson,* S. L. Gai,† and N. R. Mudford‡
Australian Defence Force Academy, Canberra ACT 2600, Australia

The results of an experimental investigation of high-enthalpy, hypersonic flow over sharp leading-edge compression corners are presented and discussed. In particular, the possible effects of real gas behavior are examined. Measurements have been made of the heat transfer and pressure distributions for flat plate and compression corner flow. Some flow visualization data have also been obtained. Test flows were generated using a free-piston shock tunnel operating in the reflected mode. The reservoir enthalpy ranged from 3 to 19 MJ kg^{-1}, giving freestream speeds of 2.3–5.5 km s^{-1}. For these conditions, the flow remains laminar throughout. The flat plate data for both high- and low-enthalpy flows are in agreement with the reference enthalpy method for heat transfer and the weak interaction theory for pressure. Also, the measured flat plate boundary-layer thickness compares well with an expression strictly valid for perfect gas flows only. The high- and low-enthalpy compression corner flows have upstream influence and plateau pressure behavior similar to perfect gas flow. That is, real gas effects for the present flows appear to be negligible. This is consistent with the essentially chemically frozen viscous and inviscid flow upstream of the interaction.

Nomenclature

C	= Chapman–Rubesin constant, $(\mu/\mu_\infty)(T_\infty/T)$
$C_{p,p}$	= plateau pressure coefficient
d	= leading-edge thickness
h	= enthalpy
h_r	= recovery enthalpy, $h_0 + 0.5(Pr^{1/2} - 1)u_\infty^2$
L	= upstream plate fetch
l_c	= upstream extent of separation
l_u	= upstream influence
l_s	= length of separated region
M	= Mach number
m	= pressure gradient parameter
Pr	= Prandtl number
p	= pressure
q_w	= heat transfer
Re_x	= Reynolds number based on distance x, $\rho_\infty u_\infty x/\mu_\infty$
Re_∞	= unit Reynolds number, $\rho_\infty u_\infty/\mu_\infty$
St	= Stanton number, $q_w/\rho_\infty u_\infty(h_r - h_w)$
T	= temperature
u	= velocity
x	= distance from leading edge
α_N	= nitrogen dissociation fraction
α_o	= oxygen dissociation fraction
δ	= boundary-layer thickness
γ_f	= frozen ratio of specific heats
θ_w	= wedge angle
ρ	= density
$(\rho ck)^{1/2}$	= thermal product
μ	= viscosity
$\bar{\chi}_L$	= hypersonic viscous interaction parameter, $M_\infty^3(C_w/Re_L)^{1/2}$

Subscripts and Superscripts

o	= at the beginning of the interaction, x_o
w	= conditions at the wall
0	= reservoir conditions
∞	= freestream conditions
$*$	= evaluated at the Eckert reference temperature

Introduction

THE flow over control surfaces and in engine inlet regions is of particular importance to re-entry and hypersonic air-breathing vehicles. The shock-wave/boundary-layer interactions that occur in these regions may result in reduced control surface effectiveness and engine performance.[1,2] The simple compression corner with an upstream flat plate and ramp (see Fig. 1) may be considered as an idealized configuration of these practical situations. The boundary layer initially develops as in flat plate flow, and some distance upstream of the corner, the ramp shock interacts with the boundary layer. For sufficiently strong shocks, the flow separates from the surface and a region of reversed flow is formed.

The hypersonic flow around re-entry vehicles will generally be chemically reactive. The majority of aerodynamic testing of compression corner flows has been conducted under low-enthalpy conditions where the flow may be treated as a perfect gas.[1] Real gas effects, such as vibration, dissociation, recombination, and ionization, may drastically alter the vehicle control and performance.[1,2] It is therefore necessary to conduct experiments under high-enthalpy conditions where real gas behavior can be simulated. It is also desirable to obtain good quality experimental data under high-enthalpy conditions so that various computational fluid dynamics (CFD) codes may be thoroughly validated.[1–3]

Compression corner flow has been studied experimentally under a wide range of low-enthalpy conditions.[4–11] For high-enthalpy flow, the experimental data are sparse,[12,13] although the general problem of high-enthalpy shock-wave/boundary-layer interaction has been considered extensively in numerical studies.[14–18] The experimental studies just quoted have only touched the surface of the problem. The

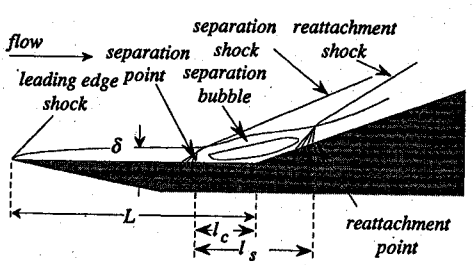

Fig. 1 Main features of compression corner flow. (Note that the leading-edge shock lies closer to the body in hypersonic flow than is shown.)

Presented as Paper 95-0155 at the AIAA 33rd Aerospace Sciences Meeting, Reno, NV, Jan. 11–14, 1995; received Feb. 24, 1995; revision received June 23, 1995; accepted for publication July 23, 1995.

*Associate Lecturer, Department of Aerospace and Mechanical Engineering, University College, University of New South Wales. Member AIAA.
†Associate Professor, Department of Aerospace and Mechanical Engineering, University College, University of New South Wales. Associate Fellow AIAA.
‡Lecturer, Department of Aerospace and Mechanical Engineering, University College, University of New South Wales.

enthalpy of the flow in the investigation by Anders and Edwards[12] was approximately 4 MJ kg^{-1}, which is too low for there to be any significant real gas effects. Stalker and Rayner[13] measured the length of the separated region in compression corner flows with enthalpies as high as 30 MJ kg^{-1} and concluded that their measurements were in agreement with theory that was strictly valid for perfect gas flow at low supersonic Mach numbers. The numerical studies[14–18] have found the size of the separated region to be reduced for flow with endothermic chemical reactions. The numerical results have not been compared with experiments due to lack of availability of suitable data. Some preliminary upstream influence data have been obtained by the present authors.[19,20] These suggest that the effect of chemical reactions on upstream influence is correctly described by the numerical studies.

This investigation considers the real gas effects on high-enthalpy compression corner flow with a sharp leading edge. Experiments were conducted in a free-piston shock tunnel that produced a range of high- and low-enthalpy conditions. Heat transfer and pressure measurements were made. Some flow visualization data were also obtained using a Mach–Zehnder interferometer.

Laminar-turbulent transition may mask any real gas effects on the flow. The present experimental conditions were chosen such that the flat plate boundary layer remained laminar. The shock-wave/boundary-layer interaction may, however, induce transition.[21–23] For all but one experiment, an examination of the heat transfer distributions for the compression corner reveals a decrease in heating upstream of the corner, consistent with laminar flow.[10] On the ramp face, the heat transfer signals do not exhibit the characteristic unsteadiness that has been previously observed in reattaching compression corner flow.[22] From these considerations, it is concluded that the flows were laminar in the present experiments.

Experimental Details

Free-Piston Shock Tunnel

The present experiments have been conducted using the Australian National University's free-piston shock tunnel facility, T3.[24,25] The reflected mode operation of the free-piston shock tunnel is shown in Fig. 2. A free piston compresses the driver gas almost isentropically. After the diaphragm bursts, the shock travels down the length of the shock tube. The shock speed is monitored by pressure transducers that are mounted in the side of the shock tube. The nozzle reservoir pressure is monitored by a transducer located just upstream of the nozzle inlet. Upon reflection from the shock tube/nozzle interface, the flow expands through the nozzle to the test section in which the experimental model is mounted.

The test time available in free-piston shock tunnels is limited by contamination of the flow by driver gas.[26] It has been shown for the T3 facility that provided the enthalpy does not exceed approximately 25 MJ kg^{-1}, there is sufficient time to establish steady flow over a flat plate.[27] It has also been shown that within these limits there is sufficient time to establish steady separated flows such as in the present experiments.[28] For this study, the steady flow periods ranged between approximately 700–1000 μs, after which any measurements were unreliable due to contamination.

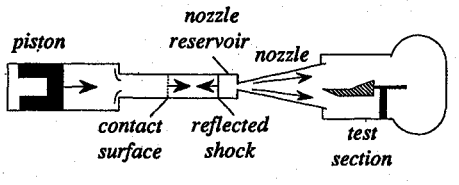

Fig. 2 Reflected mode operation of the free-piston shock tunnel.

Nozzle

The nozzle used in the present experiments was an axisymmetric conical nozzle with a throat diameter of 12.7 mm, exit diameter of 304.8 mm, and half-angle of 7.5 deg. A pitot survey of the nozzle showed the flow divergence over the model length to be approximately 1 deg. This will induce a small pressure gradient of the form $u_e \sim x^m$. The value of m was calculated using an expression from Ref. 29 and found to be approximately equal to 0.01 for all three conditions. The flow divergence effects are therefore considered small.

Calculation of Freestream Conditions

Tests were conducted at three different enthalpies: approximately 19, 14, and 3 MJ kg^{-1}. These conditions are referred to as B, D, and G, respectively.[27] The test gas was air. Conditions B, D, and G correspond to a high level of oxygen dissociation ($\alpha_o = 0.8$), a moderate level of oxygen dissociation ($\alpha_o = 0.4$), and no oxygen dissociation in the freestream, respectively. The level of freestream nitrogen dissociation was negligible ($\alpha_N < 10^{-7}$) for all conditions.

The nozzle reservoir conditions were calculated using a computer code known as ESTC.[30] This code requires as input the shock speed, nozzle reservoir pressure, and shock tube filling pressure. The first two are obtained from records of the pressure transducers mounted in the shock tube wall and have uncertainties of less than ±5%. The shock tube filling pressure is carefully monitored so that its uncertainty is negligible. ESTC calculates the reflected shock pressure and then performs an isentropic expansion to the measured reservoir pressure. Equilibrium chemistry is assumed throughout the calculations.

The nozzle exit flow conditions are calculated using a computer code known as NENZF.[31] This code requires as its input the reservoir pressure and temperature and the nozzle geometry. Measurements of the nozzle freestream temperature using coherent anti-Stokes Raman spectroscopy (CARS) have been found to compare very well with that calculated by the code.[32] NENZF performs a one-dimensional, inviscid expansion through a specified nozzle geometry. The code can calculate flows in which the gas phase reactions are considered frozen, in nonequilibrium or in equilibrium. The vibrational states can be considered either frozen at the reservoir temperature or in equilibrium. In reality, vibration will be initially highly excited and then relax along the nozzle. The Lighthill ideal dissociating gas model,[33] which is a good approximation for nitrogen and oxygen, assumes the vibrational states to be half-excited.[34] Further, the differences between the results obtained using NENZF with the equilibrium vibration assumption and the nozzle code SURF,[35] which permits a more accurate treatment of vibrational relaxation, have been found to be negligible in the present flows. The equilibrium assumption is thus the more reasonable approximation and has been adopted here.

The flow along the nozzle wall produces a boundary-layer thickness that has been measured to be approximately 25 mm for all three conditions. To account for this, the NENZF code is run until the calculated and measured pitot pressure are equal. An extensive pitot survey [36] has shown that this is equivalent to assuming an inviscid flow through a conical nozzle with half-angle 7.3 deg (conditions B and D) or 6.9 deg (condition G) up to the desired axial location. This correction has been employed in the present study.

The reservoir and freestream properties are presented in Table 1. The error due to variations in shock speed and reservoir pressure are of the same order as variations due to flow divergence over the model length. These values are for temperature ±5%, for pressure ±15%, for density ±12%, for velocity ±2%, and for Mach number ±3%. The species concentrations vary by less than 0.5%. These are of the same order as or less than the shot-to-shot repeatability.[37]

Table 1 Reservoir and freestream conditions

	h_0, MJ kg^{-1}	p_0, MPa	T_0, K	p_∞, kPa	T_∞, K	ρ_∞, gm^{-3}	u_∞, km s^{-1}	M_∞	Re_∞ × 10^{-5} m^{-1}	$\gamma_{f\infty}$	α_o
B	19.0	22.2	8400	0.99	1160	2.60	5.47	7.5	3.10	1.45	0.8
D	13.7	22.2	7200	0.99	940	3.43	4.72	7.5	4.08	1.43	0.4
G	2.83	22.4	2400	0.73	160	16.0	2.28	9.1	32.2	1.40	0.0

In the calculation of the Reynolds number, the viscosity μ was obtained from a curvefit to values calculated assuming a Lenard–Jones potential.[38] The Prandtl number does not vary appreciably over the range of conditions tested[39] and was assumed to have a constant value of 0.72. The model wall temperature was taken as 300 K (ambient).

Model Details

The models consisted of a flat plate and a ramp plate. The plates rested upon gauge housings that, in turn, were attached to a support plate. The ramp angle was adjusted by inserting wedges beneath the gauge housings. Separate models were used for the heat transfer and pressure measurements. Upwash from the undersurface of the model was prevented by side skirts. The corner formed at the junction of the two plates was set as close as possible and leakage through the corner was prevented by sealing from beneath with an industrial sealing compound. A sketch of the model is shown in Fig. 3. Although measurements have been made at a variety of compression angles, this paper will concentrate on the data for 10, 15, 18, and 24 deg as well as flat plate flow.

Studies have shown that an acceptable two-dimensional flow in the midspan region can be obtained for models without side fences and an aspect ratio of one or more.[4,5,7] A more explicit requirement was adopted in Ref. 6 where a two-dimensional flow in the midspan was said to occur only when addition of side fences and successive increases in aspect ratio did not alter the spanwise or chordwise distributions of the measured quantities.

Reference 40 employed the experimental results of Ref. 6 for code validation. Good agreement was found between a two-dimensional calculation and the experiment data for attached and incipiently separated flow. For well-separated flows, however, the two-dimensional calculation proved unsatisfactory. When a three-dimensional calculation was performed, good agreement was achieved with the experimental data for both the surface distributions and the time to establish steady separated flow.

A more recent study[41] found that a two-dimensional CFD comparison of the Ref. 6 separated flow data was as good as, if not better than, the three-dimensional calculation of Ref. 40. This does not imply that the separated flow of Ref. 6 was purely two dimensional. It does, however, seem to suggest that the midspan region may be considered a reasonable representation of two-dimensional flow if it is not affected by the addition of side fences and increases in aspect ratio, while three-dimensional effects are stronger near the end regions.

To examine the two-dimensionality of the flow in the present study, the heat transfer was measured within the separated region at off-centerline locations for flow with and without side fences.[19] These measurements compared very well with those taken on the model centerline at the same axial location. This would indicate that the flow in the model midspan was two dimensional.

The leading edge had a thickness of not greater than 10 μm, which satisfies the criterion for sharpness proposed by Stollery[42]:

$$Re_d \ll M_\infty^3 / \bar{\chi}_L^{\frac{1}{2}} \tag{1}$$

A model width of 180 mm was chosen to fit within the inviscid core of the nozzle. The sides of the plate were inclined 4.3 deg to match the source flow from the nozzle virtual origin. The model length of 180 mm ensured that it was within the nozzle Mach cone and also that it satisfied the aspect ratio requirements for two-dimensional flow. The upstream separated length is at most 10 times the boundary-layer thickness,[10] which has been measured to be approximately 3 mm for similar flow conditions to the present study.[43] The upstream and downstream separation lengths are approximately equal. Thus at least 30 mm of downstream plate is required. The ramp length was set at 95 mm to ensure reattachment is completed on the ramp face.

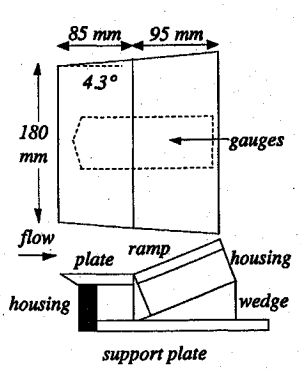

Fig. 3 Schematic of the model. (Side plates not shown.)

Instrumentation

The heat transfer was obtained using coaxial chromel-alumel (type 'K') surface junction thermocouples. These devices have been successfully employed in a number of investigations.[37,44,45] They are able to withstand the harsh environment of the free-piston shock tunnel for more than 50 shots, whereas conventional thin film gauges are typically rendered useless after a single shot.[27] The heat transfer is inferred from the variation of temperature with time as measured by the thermocouples according to the method of Ref. 46. The thermocouple thermal product was determined to be $(\rho ck)^{1/2} = 9500 \pm 500\ W\ s^{1/2}\ m^{-2}\ K^{-1}$ using the method of Ref. 47. The uncertainty in heat transfer as measured by these gauges is approximately 15%.[37]

The pressures were measured using PCB 113M165 piezoelectric pressure transducers. These were calibrated in the range 0.5–50 kPa by applying a known pressure difference to the face of the transducer. The gauge response was linear even at the lower range of the pressures.

The pressure transducers were carefully mounted to minimize transmission of stress waves along the model. The retaining screws were finger tight as this has been found to minimize stress wave transmission.[48] The transducers were recessed to protect them from the harsh environment of the shock tunnel flow. The fluctuation in signal levels during the steady flow period was approximately ±10%. This is of the same order as the accuracy to which the flow conditions in shock tunnels are known.

The gauge outputs were amplified before being digitized by a LeCroy 2264 Waveform Digitization Unit sampling at 400 kHz per channel. The system was configured to give 3.84 ms of signal after the passage of the primary shock over the first timing gauge mounted in the shock tube side wall. A personal computer was used to view the signals and to calculate the heat transfer and pressure. Typical heat transfer and pressure signals are shown in Fig. 4.

Flow visualization data were obtained using a Mach–Zehnder interferometer. The light source was a flashlamp pumped dye laser with a wavelength of 589.1 ±0.6 nm. The laser pulse length was typically 1 μs. The interferograms may be analyzed to yield the phase distribution in a manner described in Refs. 49 and 50. The thermal boundary-layer thickness may be obtained by examining the profile normal to the surface. The boundary-layer thickness may then be obtained from[51]

$$\frac{\delta}{\delta_{\text{thermal}}} \approx Pr^{\frac{1}{2}} \tag{2}$$

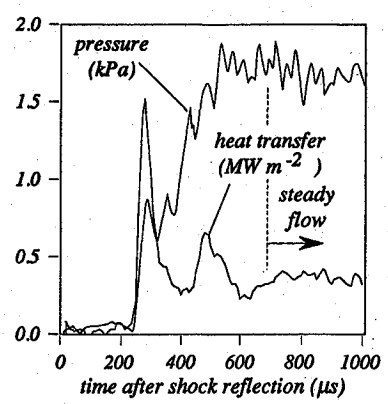

Fig. 4 Examples of heat transfer and pressure traces for h_0 = 19 MJ kg^{-1}.

Results

Flat Plate (θ_w = 0 deg)

The configuration where the corner angle is zero is equivalent to a flat plate and is the datum for compression corner flow. Figure 5 shows the heat transfer data pertaining to this geometry. Also shown are the reference enthalpy predictions that include the effect of freestream dissociation.[27] Although the comparison can be considered reasonable in general, the data scatter is quite large, particularly at the lowest enthalpy. This is mainly due to poor signal-to-noise ratio at this condition.

The pressure distributions are shown in Fig. 6. Also shown in Fig. 6 is the weak interaction prediction[52] that compares well with the data. As mentioned earlier, the pressure gradient due to the conical nature of the flow was small, and from this figure, it would not seem to have significantly affected the results.

The flat plate boundary-layer thickness distribution determined from the phase distributions is presented for conditions B, D, and G in Fig. 7. Also shown are values calculated using an expression

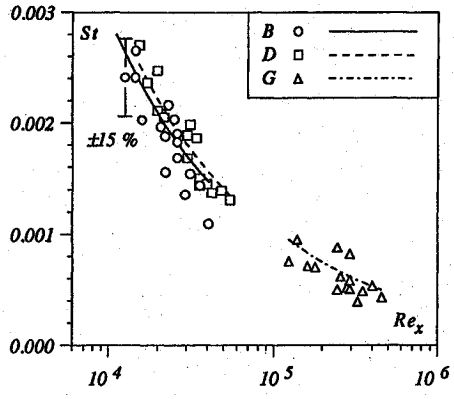

Fig. 5 Flat plate heat transfer distributions. (Symbols denote experiment, curves denote theory.)

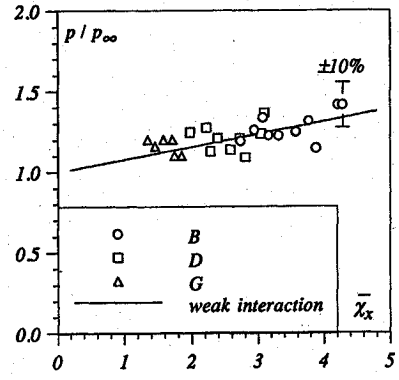

Fig. 6 Flat plate pressure distributions. (Symbols denote experiment, curve denotes theory.)

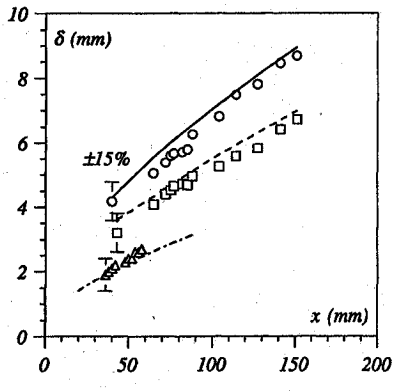

Fig. 7 Flat plate boundary-layer thickness distribution (see Fig. 5 for explanation of symbols).

derived for flat plate laminar boundary-layer thickness of a perfect gas[36]:

$$\frac{\delta}{x} = \frac{1.721}{\sqrt{Re_x}}\left\{2.39 + \frac{T_w}{T_e} + 0.097 Pr^{\frac{1}{2}}(\gamma - 1)M_e^2\right\} \qquad (3)$$

The condition G data were taken upstream of the corner from an interferogram with the wedge angle set at θ_w = 15 deg. Thus the data for this conditions are sparse. The high- and low-enthalpy data are in good agreement with the perfect gas expression. That is, the test gas in the flat plate boundary layer seems to behave like a perfect gas for both high- and low-enthalpy conditions.

Compression Corner ($\theta_w > 0$ deg)

The heat transfer and pressure distributions are shown in Figs. 8 and 9, respectively, for the three flow conditions with wedge angles of 10, 15, 18, and 24 deg. The wedge angle for the heat transfer data for condition G at 15 deg was actually obtained at 14 deg. The differences between 14 and 15 deg are expected to be small.

As the wedge angle is increased, the interaction feeds forward and the values of heat transfer and pressure on the ramp increase.

The pressure gradient due to the corner shock causes the heat transfer to decrease and the pressure to increase upstream of the

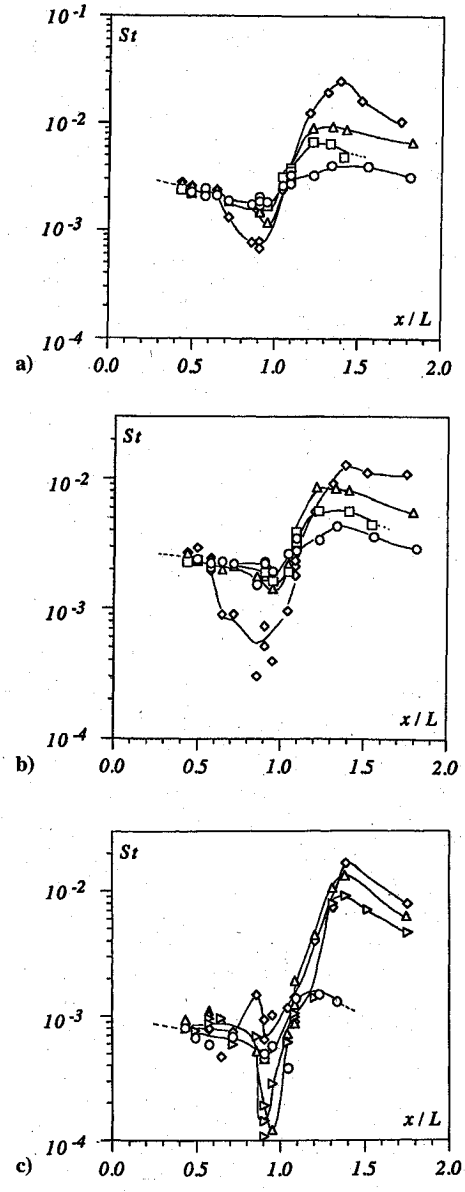

Fig. 8 Heat transfer distributions for $\theta_w > 0$ deg: ○, 10 deg; ▷, 14 deg; □, 15 deg; △, 18 deg; ◇, 24 deg: a) condition B, b) condition D, and c) condition G.

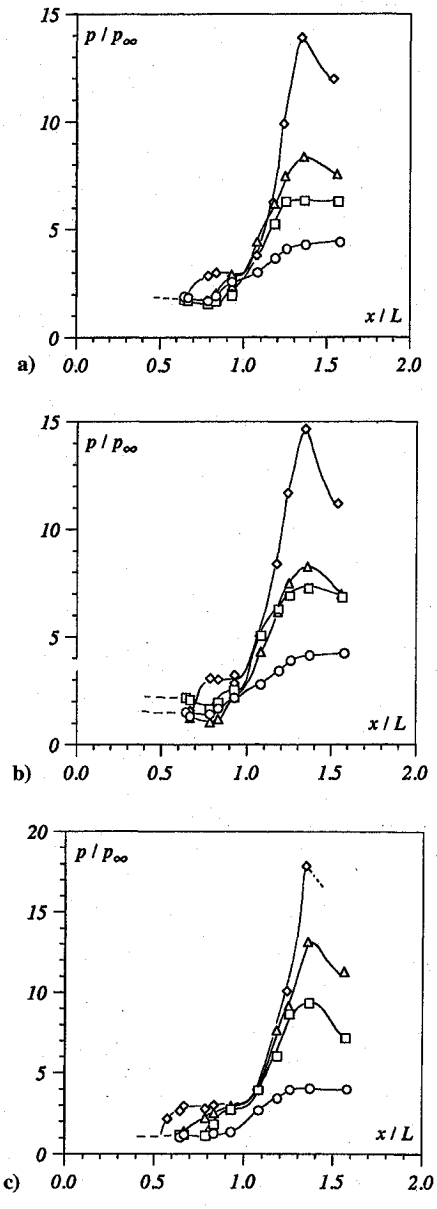

Fig. 9 Pressure distributions for $\theta_w > 0$ deg: a) condition B, b) condition D, and c) condition G (see Fig. 8 for explanation of symbols).

corner. The general characteristics of heat transfer and pressure distributions in the presence of strong adverse pressure gradients are well known.[9,10] For attached flow the heat transfer minimum is sharp and the pressure rise is continuous. For incipiently separated flow, the heat transfer minimum is slightly rounded and an inflexion appears on the pressure distribution curve. For fully separated flow, the heat transfer minimum is well rounded and plateau in the pressure distribution straddles the corner.

Based on these descriptions, for a corner angle of 10 deg, the flow is attached for all flow conditions. For a corner angle of 15 deg, the flow is attached for conditions B and D whereas it appears to be incipiently separated for G. For a corner angle of 18 deg, the flow is incipiently separated for conditions B and D and well separated for G. The flow is well separated for all of the flow conditions for a corner angle of 24 deg.

The heat transfer for condition G, $\theta_w = 24$ deg, appears to rise slightly just upstream of the corner, indicating possible flow transition to turbulence. The high Mach and low Reynolds numbers for condition G make this unlikely. Also, as mentioned earlier, the heat transfer signals on the ramp do not exhibit any characteristic unsteadiness as observed in transitional compression corner flows.[22] The rise is more probably an indication of the scatter in heat transfer data for condition G due to poor signal-to-noise ratio.

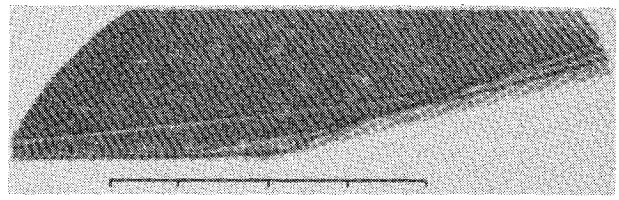

Fig. 10 Interferogram for condition G, $\theta_w = 15$ deg. Flow is from left to right.

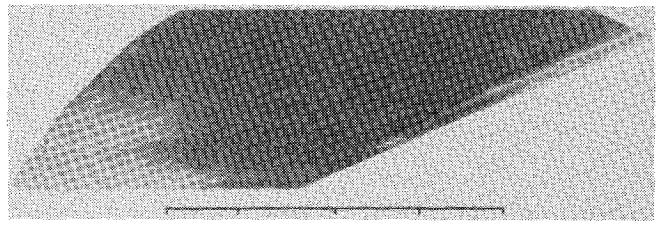

Fig. 11 Interferogram for condition B, $\theta_w = 24$ deg. Flow is from left to right.

The distinction between incipient and fully separated conditions is not very clear for condition G. The flow visualization for condition G at $\theta_w = 15$ deg is shown in Fig. 10. A small region of separated flow near the corner can be seen. This would indicate that the flow is just past the incipient separation condition. Figure 10 also shows the shock/shock interactions that are a common feature of hypersonic compression corner flow. For comparison, the infinite fringe interferogram for separated ($\theta_w = 24$ deg) flow for condition B is shown in Fig. 11. The fringes in an infinite fringe interferogram are representative of the density contours. A large separated region and shock/shock interaction are evident in Fig. 11.

Upstream Influence

For a considerable distance downstream of the leading edge, the heat transfer and pressure are identical to that for flat plate flow. The upstream influence may be defined as the distance from the corner at which the heat transfer and pressure first deviate from the flat plate values. This is of the same order as the upstream extent of separation. The separation point may be determined from flow visualization, pressure distributions, or skin-friction distributions. Flow visualization data are not always available, and the method of determining the separation point from a pressure distribution is prone to error. The third of these methods is the most preferable as the separation point is defined as the location of zero skin friction. For hypersonic flows, skin friction has always proved difficult to measure. Progress has been made in this field for free-piston shock tunnel flows[53] but the methods have not been proven in reversed flows. Therefore, the upstream influence is a useful way of characterising the length of the separated region.

The upstream length of separation and upstream influence increase with increasing Reynolds number, wedge angle, boundary-layer thickness (for hypersonic flows, the boundary-layer thickness and the displacement thickness are approximately equal[54] and both may be used to scale the upstream influence[10]), and wall-to-total temperature ratio and decreasing Mach number.[5,7,9,10,55,56] The upstream influence may therefore be expressed as

$$l_u = F\left(Re_{x_o}, \theta_w, \delta(x_o), T_w/T_0, M_o\right) \tag{4}$$

where the properties are evaluated just upstream of the interaction at x_o.

Needham and Stollery[56] noted that the length of the separated region normalized by the boundary-layer thickness is independent of the wall-to-adiabatic-wall temperature ratio. This ratio varies in a similar manner to the wall-to-total temperature ratio. Thus, the upstream influence may be simplified to

$$l_u/\delta = F\left(Re_{x_o}, \theta_w, M_o\right) \tag{5}$$

Stollery[57] noted that $(M_\infty \theta_w)^2/A\bar{\chi}$, where $A = (\gamma - 1)(0.332 + 0.865T_w/T_0)$ is the governing parameter for flow over a sharp flat

plate at incidence in hypersonic flow. It is therefore tempting to rewrite Eq. (5) as

$$\frac{l_u}{\delta} = F\left\{\frac{(M_o\theta_w)^2}{\bar{\chi}_o}\right\} \tag{6}$$

where the fact that l_u/δ is independent of the wall-to-total temperature ratio results in the absence of A in Eq. (6). It is interesting to note that the incipient separation condition as given in Refs. 9 and 10 is of the same form as Eq. (6).

Katzer[58] found the length of the separated region for supersonic flow to be given by

$$\frac{l_{sep}}{\delta} = 4.4\frac{\Delta p}{p(x_o)}\frac{\left(Re_{x_o}/C^*\right)^{\frac{1}{2}}}{M_o^3} \tag{7}$$

where Δp is the pressure rise from separation to the final value achieved at reattachment. The exact method used to derive this expression was not stated, but it would appear to have been obtained from an analysis based on the free interaction near separation. Katzer did not choose to simplify the second ratio in Eq. (7) to the hypersonic interaction parameter as the study focused on supersonic flows. For the present purposes, the simplification is in order. The pressure ratio $\Delta p/p_{x_o}$ may be approximated using the tangent wedge formula,[52] so that

$$\frac{\Delta p}{p(x_o)} \approx (M_o\,\theta_w)^2 \tag{8}$$

For hypersonic flows, the length of the separated region is then given as

$$\frac{l_{sep}}{\delta} \approx \frac{(M_o\,\theta_w)^2}{\bar{\chi}_o} \tag{9}$$

which is the same as the functional relationship for the upstream influence expressed in Eq (6).

At high enthalpy, nonequilibrium vibrational excitation and chemical reaction may affect the separated length through a change in shock angle, a change in boundary-layer thickness, and relaxation effects in the reversed flow region.

The shock angle may be reduced thereby decreasing the pressure rise. The distance required for this to happen, however, would be many body lengths. Significant nonequilibrium effects of this nature are to be expected only for wedge angles much larger than those used here.[59] Even then,the difference between frozen and equilibrium shock angles is only a few degrees,[60,61] and so the effect on the pressure would be small.

The boundary-layer thickness for nonequilibrium flow differs from the perfect gas value by an amount that depends upon the level of nonequilibrium in the boundary layer.[36] For dissociation dominated boundary-layer flow, the boundary-layer thickness would be reduced, whereas for recombination-dominated flow,the thickness would be increased. According to Eq. (6), this would mean the upstream influence and length of the separated region would be reduced for dissociation-dominated flows and increased for recombination-dominated flows. The high-enthalpy boundary-layer flows in the present study were found to be essentially chemically frozen. This means that the upstream influence should not be significantly affected by nonequilibrium vibrational excitation and chemical reactions in the boundary layer for the present high-enthalpy conditions.

If the length scale for the nonequilibrium chemical processes, l_{chem}, is of the same order as the scale of the separated region, then it becomes an additional variable in Eq. (6). For frozen flow, reactions proceed more slowly than the characteristic flow time and $l_{chem}/\delta \to \infty$. For equilibrium flow, reactions proceed faster than the characteristic flow time and $l_{chem}/\delta \to 0$. The chemical length scale is therefore not a determining variable for extent of the separated region when the flow is frozen or in equilibrium. When the flow is in equilibrium, the length of the separated region will still be affected by the change in boundary-layer thickness as detailed in the previous paragraph. The boundary layer for the present high-enthalpy conditions is essentially chemically frozen, which indicates that the chemical length scale is much larger than the boundary-layer thickness. Thus, it is not expected that relaxation would affect the length of the separated region.

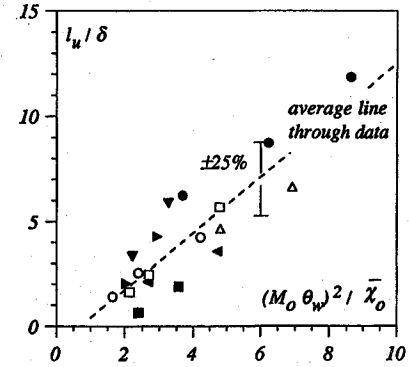

Fig. 12 Upstream influence in hypersonic laminar compression corner flow: ○, B; □, D; △, G; ■, Ref. 4; ▼, Ref. 5 ◄, Ref. 6; ►, Ref. 8; and ●, Ref. 56.

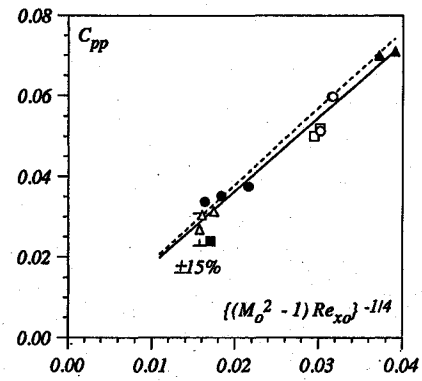

Fig. 13 Plateau pressue for high- and low-enthalpy flow (symbols denote experiment, curves denote theory): ○, B; □, D; △, G; •, Ref. 5; ■, Ref. 6, ◄, Ref. 8; and ▲, Ref. 62; ——, Ref. 62; and - - - -, Ref. 63.

The upstream influence for separated flows for conditions B, D, and G are compared in Fig. 12 using the form of Eq. (6). Also shown are the perfect gas data from Refs. 4–6, 8, and 56, along with an average line through the data. The data from the other experiments are known to be for laminar flow throughout the separated region. The flow was deemed separated if either the pressure distribution had a plateau, the heat transfer showed a rounded minimum, the skin friction decreased below zero, or the flow visualization revealed a separated region. The high- and low-enthalpy data from the present experiments correlate well in this form as do the perfect gas data from the other experiments. That is, the high-enthalpy flows appear to behave as a perfect gas. The observation from a previous study[20] that the upstream influence in the present high-enthalpy flows was less than that for perfect gas flows was due to use of an incorrect correlating parameter.

Pressure Rise to Plateau

Another important parameter in shock-wave/boundary-layer interaction is the so called plateau pressure. The plateau pressure in supersonic shock-wave/boundary-layer interactions is given by a number of investigations as

$$C_{p,p} = k\left(M_o^2 - 1\right)^{-\frac{1}{4}} Re_{x_o}^{-\frac{1}{4}} \tag{10}$$

where k is a constant. Values for k include 1.82 (Ref. 62) and 1.90 (Ref. 63). Equation (10) has been found to compare well with plateau pressure data from hypersonic flow over a forward-facing step.[55]

Data from the present experiments are shown in Fig. 13 along with perfect gas experimental data from Refs. 5, 6, and 62 and the theoretical values from Refs. 62 and 63. The high- and low-enthalpy data compare well with the theory, Eq. (10), which indicates that the high-enthalpy flows behave as a perfect gas flow for the present experiments.

Conclusions and Summary

High-enthalpy, laminar, hypersonic compression corner flow has been investigated for a range of attached and separated flows. The results may be summarized as follows.

Flat Plate Flow

The flat plate data compare favorably with the reference enthalpy method for heat transfer, the weak interaction result for pressure, and a perfect gas laminar flow expression for the boundary-layer thickness. This suggests that the flow is laminar and frozen and behaves as a perfect gas for the present high- and low-enthalpy conditions.

Compression Corner Flow

1) The heat transfer and pressure on the face of the ramp and the upstream influence were found to increase with increasing wedge angle.

2) An expression for the upstream influence in perfect gas flows has been developed. This expression correlated the high- and low-enthalpy data from the present study quite well. Data from previous laminar compression corner flow experiments also correlated well with the present data and according to the new expression.

3) The plateau pressure for high- and low-enthalpy flows was found to be well described by an expression for perfect gas flows derived from the concept of a free interaction in laminar supersonic flow.

The main conclusion to be drawn from these results is that in spite of the flow enthalpies being sufficient for chemical reaction, the real gas effects are negligible for the present experimental flow conditions and model dimensions. Clearly, larger models exposed to flows with higher enthalpies would be required to investigate the possible effects of real gas behavior in this type of flow. Higher enthalpy flows as generated by free-piston shock tunnels seem to have large proportions of driver gas in the test flows. Higher enthalpies may also be generated by free-piston expansion tubes, but these have small test times, and so it is unlikely that steady separated flow could be established. Until these problems are addressed, an experimental investigation where real gas effects are prominent in compression corner flows remains a distant possibility.

Acknowledgments

The authors would like to thank P. M. Walsh for assistance with the experiments, J. W. Morton for advice on the flow visualization and interferogram analysis, and the Department of Physics and Theoretical Physics, Australian National University, for providing the interferogram analysis package.

References

[1]Neumann, R. D., "Experimental Methods for Hypersonics: Capabilities and Limitations," Lecture Notes, 2nd Joint Europe/U.S. Short Course on Hypersonics, U.S. Air Force Academy (Colorado Springs, CO), Birkhäuser, Boston, Jan. 1989.

[2]Park, C., *Nonequilibrium Hypersonic Aerothermodynamics*, Wiley, New York, 1990.

[3]Désidéri, J.-A., Glowinski, R., and Périaux, J., *Hypersonic Flows for Reentry Problems*, Vol. 1, Springer–Verlag, Berlin, 1991.

[4]Holden, M. S., "Theoretical and Experimental Studies of Laminar Flow Separation on Flat Plate-Wedge Compression Surfaces in the Hypersonic Strong Interaction Regime," Aeronautical Research Lab., ARL Rept. 67-0112, Wright–Patterson AFB, OH, 1967.

[5]Lewis, J. E., Kubota, T., and Lees, L., "Experimental Investigation of Supersonic Laminar, Two-Dimensional Boundary-Layer Separation in a Compression Corner with and Without Cooling," *AIAA Journal*, Vol. 6, No. 1, 1968, pp. 7–14.

[6]Holden, M. S., and Moselle, J. R., "Theoretical and Experimental Studies of the Shock Wave-Boundary Layer Interaction on Compression Surfaces in Hypersonic Flow," Aeronautical Research Lab., ARL Rept. 70-0002, Wright–Patterson AFB, OH, 1970.

[7]Miller, D. S., Hijman, R., and Childs, M. E., "Mach 8 to 22 Studies of Flow Separations Due to Deflected Control Surfaces," *AIAA Journal*, Vol. 2, No. 2, 1964, pp. 312–321.

[8]Bloy, A. W., and Georgeff, M. P., "The Hypersonic Laminar Boundary Layer Near Sharp Compression and Expansion Corners," *Journal of Fluid Mechanics*, Vol. 63, 1974, pp. 431–447.

[9]Hankey, W. L., Jr., and Holden, M. S., "Two Dimensional Shock Wave-Boundary Layer Interactions in High Speed Flows," AGARDograph 203, 1975.

[10]Délery, J., "Shock/Shock and Shock-Wave/Boundary-Layer Interactions in Hypersonic Flows," AGARD Rept. 761, Pt. 9, June 1989.

[11]Simeonides, G., Haase, W., and Manna, M., "Experimental, Analytical, and Computational Methods Applied to Hypersonic Compression Ramp Flows," *AIAA Journal*, Vol. 32, No. 2, 1994, pp. 301–310.

[12]Anders, J. B., and Edwards, C. L. W., "A Real-Gas Study of Low-Density Wedge-Induced Laminar Separation on a Highly Cooled Blunt Flat Plate at $M_\infty = 12$," NASA TN D-4320, March 1968.

[13]Stalker, R. J., and Rayner, J. P., "Shock Wave-Laminar Boundary Layer Interaction at Finite Span Compression Corners," *Proceedings of the 15th International Symposium on Shock Waves and Shock Tubes*, Stanford Univ. Press, Stanford, CA, 1985, pp. 509–515.

[14]Brenner, G., and Prinz, U., "Numerical Simulation of Chemical and Thermal Nonequilibrium Flows After Compression Shocks," AIAA Paper 92-2879, July 1992.

[15]Brenner, G., Gerhold, T., Hannemann, K., and Rues, D., "Numerical Study of Shock/Shock and Shock-Wave/Boundary-Layer Interactions in Hypersonic Flows," *Computers and Fluids Journal*, Vol. 22, No. 4/5, 1993, pp. 427–439.

[16]Ballaro, C. A., and Anderson, J. D., Jr., "Shock Strength Effects on Separated Flows in Non-Equilibrium Chemically Reacting Air Shock Wave/Boundary Layer Interaction," AIAA Paper 91-0250, Jan. 1991.

[17]Grasso, F., and Leone, G., "Chemistry Effects in Shock Wave Boundary Layer Interaction," *Proceedings of the IUTAM Symposium: Aerothermochemistry of Spacecraft and Associated Hypersonic Flows* (Marseille, France), Jouve, Paris, 1992, pp. 220–227.

[18]Grumet, A., Anderson, J. D., Jr., and Lewis, M. J., "Numerical Study of the Effects of Wall Catalysis on Shock Wave/Boundary Layer Interaction," *Journal of Thermophysics and Heat Transfer*, Vol. 8, No. 1, 1994, pp. 40–47.

[19]Mallinson, S. G., Gai, S. L., and Mudford, N. R., "Laminar Flows of High Enthalpy Air in a Compression Corner," *Proceedings of the 11th Australasian Fluid Mechanics Conference* (Hobart, Tasmania), Univ. of Tasmania Press, Hobart, Australia, 1992, pp. 275–278.

[20]Mallinson, S. G., Gai, S. L., and Mudford, N. R., "Shock Wave/Boundary Layer Interaction in High Enthalpy Compression Corner Flow," *Proceedings of the 19th International Symposium on Shock Waves* (Université de Provence, Marseille), Vol. 1, Springer–Verlag, Berlin, 1993, pp. 87–92.

[21]Zheltovodov, A. A., Pavlov, A. A., Shilein, E. H., and Yakovlev, V. N., "Interconnectionship Between the Flow Separation and the Direct and Inverse Transition at Supersonic Speed Conditions," *Proceedings of the IUTAM Symposium: Laminar-Turbulent Transition* (Novosibirisk, USSR), Springer–Verlag, Berlin, 1985, pp. 503–508.

[22]Kumar, D., and Stollery, J. L., "Effects of Leading Edge Bluntness on Control Flap Effectiveness at Hypersonic Speeds," *Proceedings of 19th International Symposium on Shock Waves* (Université de Provence, Marseille), Vol. 1, Springer–Verlag, Berlin, 1993, pp. 47–52.

[23]Kumar, D., and Stollery, J. L., "Hypersonic Control Flap Effectiveness," 19th ICAS Congress, International Council of the Aeronautical Sciences, ICAS Paper 94-4.4.3, 1994.

[24]Stalker, R. J., "Development of a Hypervelocity Wind Tunnel," *Aeronautical Journal*, Vol. 76, 1972, pp. 374–384.

[25]Gai, S. L., "Free Piston Shock Tunnels: Developments and Capabilities," *Progress in Aerospace Science*, Vol. 29, No. 1, 1992, pp. 1–41.

[26]Crane, K. C. A., and Stalker, R. J., "Mass-Spectrometric Analysis of Hypersonic Flows," *Journal of Physics D: Applied Physics*, Vol. 10, No. 5, 1977, pp. 679–695.

[27]East, R. A., Stalker, R. J., and Baird, J. P., "Measurements of Heat Transfer to a Flat Plate in a Dissociated High-Enthalpy Laminar Air Flow," *Journal of Fluid Mechanics*, Vol. 97, No. 4, 1980, pp. 673–699.

[28]Mallinson, S. G., and Gai, S. L., "Establishment of Laminar Separated Flows in a Free-Piston Shock Tunnel," *Proceedings of the IUTAM Symposium: Aerothermochemistry of Spacecraft and Associated Hypersonic Flows* (Marseille, France), Jouve, Paris, 1992, pp. 368–373.

[29]Cohen, C. G., and Reshotko, E., "Similar Solutions for the Compressible Laminar Boundary Layer with Heat Transfer and Pressure Gradient," NACA Rept. 1293, 1956.

[30]McIntosh, M. K., "Computer Program for the Numerical Calculation of Frozen and Equilibrium Conditions in Shock Tunnels," Internal Rept., Dept. of Physics, Faculties, Australian National Univ., 1968.

[31]Lordi, J. A., Mates, R. E., and Moselle, J. R., "Computer Program for the Numerical Solution of Nonequilibrium Expansions of Reacting Gas Mixtures," NASA CR-472, 1966.

[32]Pulford, D. R. N., Newman, D. S., Houwing, A. F. P., and Sandeman, R. J., "Temperature Measurements Using Coherent Anti-Stokes Raman Scattering in a Pulsed High Enthalpy Supersonic Flow," *Proceedings of the IUTAM Symposium: Aerothermochemistry of Spacecraft and Associated Hypersonic Flows* (Marseille, France), Jouve, Paris, 1992, pp. 469–474.

[33]Lighthill, M. J., "Dynamics of a Dissociating Gas. Part I, Equilibrium Flow," *Journal of Fluid Mechanics*, Vol. 2, 1957, pp. 1–32.

[34]Vincenti, W. G., and Kruger, C. H., *Introduction to Physical Gasdynamics*, Wiley, New York, 1965.

[35]Rein, M., "Surf: A Program for Calculating Inviscid Supersonic Reacting Flows in Nozzles," Graduate Aeronautical Labs., California Inst. of Technology, GALCIT TR FM 89-1, Pasadena, CA, 1989.

[36]Mallinson, S. G., "Shock Wave/Boundary Layer Interaction at a Compression Corner in Hypervelocity Flows," Ph.D. Thesis, Univ. of New South Wales, Canberra, Australia, 1994.

[37]Gai, S. L., and Joe, W. S., "Laminar Heat Transfer to Blunt Cones in High-Enthalpy Hypervelocity Flows," *Journal of Thermophysics and Heat Transfer*, Vol. 6, No. 3, 1992, pp. 433–438.

[38]Hirschfelder, J. O., Curtiss, C. F., and Bird, R. B., *Molecular Theory of Gases and Liquids*, 4th ed., Wiley, New York, 1967.

[39]Hansen, C. F., "Approximations for the Thermodynamic and Transport Properties of High Temperature Air," NASA TR R-50, 1959.

[40]Rudy, D. H., Thomas, J. L., Kumar, A., Gnoffo, P. A., and Chakravarthy, S. R., "Computation of Laminar Hypersonic Compression-Corner Flows," *AIAA Journal*, Vol. 29, No. 7, 1991, pp. 1108–1113.

[41]Lee, J. Y., and Lewis, M. J., "Numerical Study of the Flow Establishment Time in Hypersonic Shock Tunnels," *Journal of Spacecraft and Rockets*, Vol. 30, No. 2, 1993, pp. 152–163.

[42]Stollery, J. L., "Viscous Interaction Effects on Re-Entry Aerothermodynamics: Theory and Experimental Results," AGARD Lecture Series 42, Vol. 1, 1972.

[43]Gai, S. L., Reynolds, N. T., Ross, C., and Baird, J. P., "Measurements of Heat Transfer in Separated High-Enthalpy Dissociated Laminar Hypersonic Flow Behind a Step," *Journal of Fluid Mechanics*, Vol. 199, 1989, pp. 541–561.

[44]Gai, S. L., Mudford, N. R., and Hackett, C., "Heat Flux and Shock Shape Measurements on an Aeroassist Flight Experiment Model in a High Enthalpy Free Piston Shock Tunnel," AIAA Paper 92-3907, July 1992.

[45]Boyce, R. R., "Computational Fluid Dynamics Code Validation Using a Free Piston Shock Tunnel," Ph.D. Thesis, Dept. of Physics and Theoretical Physics, Faculties, Australian National Univ., Canberra, Australia, 1995.

[46]Schultz, D. L., and Jones, T. V., "Heat-Transfer Measurements in Short-Duration Hypersonic Facilities," AGARDograph 165, Feb. 1973.

[47]Jessen, C., Vetter, M., and Grönig, H., "Experimental Studies in the Aachen Hypersonic Shock Tunnel," *Zeitschrift für Flugwissenschaften und Weltraumforschung*, Vol. 17, No. 2, 1993, pp. 73–81.

[48]Stacey, C. H. B., "Swept Shock Wave/Boundary Layer Interactions at High Mach Number," Ph.D. Thesis, Dept. of Mechanical Engineering, Univ. of Queensland, Brisbane, Australia, 1989.

[49]Bone, D. J., "A Users Guide to FrAnSys—A Fringe Analysis System," Internal Rept., Dept. of Physics and Theoretical Physics, Faculties, Australian National Univ., 1991.

[50]Boyce, R. R., Morton, J. W., Houwing, A. F. P., Mundt, C., and Bone, D. J., "CFD Validation Using Multiple Interferometric Views of Three Dimensional Shock Layer Flows over a Blunt Body," AIAA Paper 94-0282, Jan. 1994.

[51]Dorrance, W. H., *Viscous Hypersonic Flow*, McGraw–Hill, New York, 1962.

[52]Anderson, J. D., Jr., *Hypersonic and High Temperature Gas Dynamics*, McGraw–Hill, New York, 1989.

[53]Kelly, G. M., "A Study of Reynolds Analogy in Hypersonic Boundary Layer Using a New Skin Friction Gauge," Ph.D. Thesis, Dept. of Mechanical Engineering, Univ. of Queensland, Brisbane, Australia, 1993.

[54]Messiter, A. F., and Matarrese, M. D., "Strip Blowing from a Wedge at Hypersonic Speeds," *AIAA Journal*, Vol. 33, No. 5, 1995, pp. 843–850.

[55]Sterrett, J. R., and Emery, J. C., "Extension of Boundary-Layer-Separation Criteria to a Mach Number of 6.5 by Utilizing Flat Plates with Forward-Facing Steps," NASA TN D-618, 1960.

[56]Needham, D. A., and Stollery, J. L., "Hypersonic Studies of Incipient Separation and Separated Flows," AGARD CP, Vol. 4, Pt. 1, 1966, pp. 89–119.

[57]Stollery, J. L., "Hypersonic Viscous Interaction on Curved Surfaces," *Journal of Fluid Mechanics*, Vol. 43, No. 3, 1970, pp. 497–511.

[58]Katzer, E., "On the Lengthscales of Laminar Shock/Boundary-Layer Interaction," *Journal of Fluid Mechanics*, Vol. 206, 1989, pp. 477–496.

[59]Kewley, D. J., and Hornung, H. G., "Non-Equilibrium Dissociating Nitrogen Flow over a Wedge," *Journal of Fluid Mechanics*, Vol. 64, No. 4, 1974, pp. 725–736.

[60]Capiaux, R., and Washington, M., "Nonequilibrium Flow Past a Wedge," *AIAA Journal*, Vol. 1, No. 3, 1963, pp. 650–660.

[61]Pandolfi, M., Arina, R., and Botta, N., "Nonequilibrium Hypersonic Flows over Corners," *AIAA Journal*, Vol. 29, No. 2, 1991, pp. 235–241.

[62]Chapman, D. R., Kuehn, D. M., and Larson, H. K., "Investigation of Separated Flows in Supersonic and Subsonic Streams with Emphasis on the Effect of Transition," NACA Rept. 1356, 1958.

[63]Hakkinen, R. J., Greber, I., Trilling, L., and Abarbanel, S. S., "The Interaction of an Oblique Shock Wave with a Laminar Boundary Layer," NASA Memo. 2-18-59W, 1959.